

NOVEMBER 1981

LRP 198/81

LARGE AMPLITUDE SOLUTIONS OF THE NONLINEAR WAVE  
EQUATION FOR AN IDEAL, COLD THREE-FLUID PLASMA

M.C. Festeau-Barrioz and E.S. Weibel

# LARGE AMPLITUDE SOLUTIONS OF THE NONLINEAR WAVE EQUATION FOR AN IDEAL, COLD THREE-FLUID PLASMA

M.C. Festeau-Barrioz and E.S. Weibel

Centre de Recherches en Physique des Plasmas  
Association Euratom - Confédération Suisse  
Ecole Polytechnique Fédérale de Lausanne  
CH-1007 Lausanne / Switzerland

## ABSTRACT

A method for obtaining numerical solutions of the nonlinear eigenvalue problem

$$\vec{\mathcal{E}}(\vec{E}) \vec{E} - \lambda \vec{\nabla} \times (\vec{\nabla} \times \vec{E}) = 0$$

is described. The nonlinearity is due to the ponderomotive force exerted by the wave on a plasma, which modifies the densities. A centred finite-difference scheme is used, which avoids spectral pollution. Starting from the linear, small amplitude solution, a predictor-corrector method allows to reach solution of increasing amplitude.

## 1. INTRODUCTION

This paper concerns the determination of suitable wave configurations for isotope separation, in a two-ion species magnetised plasma. In a previous paper [1], we investigated the case of the left-hand circularly-polarised wave, travelling within an infinite plasma. More recently [2], we extended our survey to modes propagating into a plasma bounded by a cylindrical conducting shell of finite length, terminated by end plates. The method of iteration used in that paper resulted in very slow convergence, making it impossible to find large amplitude modifications.

The second section of this paper is devoted to a speedy statement of the physical problems. We present, in the third section, the two important features of our numerical solution, one is the finite-difference scheme that weeds out the undesirable modes from the operator's spectrum, the second one is a predictor-corrector method which improves largely the quality of the convergence. The fourth section is dedicated to the results obtained with the above-mentioned process. We shall use, in this report, cylindrical coordinates  $(r, \phi, z)$ , and natural units [3], except for the physical results that will be given in MKS units.

## 2. THE NONLINEAR WAVE EQUATION

An important nonlinear phenomenon in plasma physics lies in the ponderomotive force, that is the radiation pressure that waves exert on charged particles. The main effect of this force is to push and bunch the particles near the loops or the nodes of the wave, causing modifications of the index of refraction.

Consider a two-ion species plasma, quasi-neutral bounded by a conducting cylinder, subject to a constant magnetic field  $B_0$ , whose direction coincides with the z-axis.

Let us choose for the amplitude of an electromagnetic wave travelling in the plasma

$$\vec{E} = [E_r(r, z), E_\phi(r, z), E_z(r, z)] e^{i(\nu\phi - \omega t)} \quad (1)$$

where  $\nu$  is an integer.

The ponderomotive force acting on species  $j$  is the gradient of a potential  $\psi_j$  [4]:

$$\vec{F}_j = - \vec{\nabla} \psi_j \quad (2)$$

$$\psi_j = \frac{q_j^2}{2m_j \omega} \left( \frac{E_L^2}{\omega - \Omega_j} + \frac{E_R^2}{\omega + \Omega_j} + \frac{E_z^2}{\omega} \right) \quad (3)$$

where:

$q_j$ : particle charge of species  $j$

$m_j$ : particle mass of species  $j$

$\omega$  : frequency of the wave

$\Omega_j$ : cyclotron frequency of species  $j$

$$E_{R,L} = \frac{1}{\sqrt{2}} \left( E_r \pm i E_\phi \right) \quad (4)$$

From the expression of  $\psi_j$ , we can immediately see that the sign of the ponderomotive force depends on whether

$$\omega \begin{matrix} < \\ = \\ > \end{matrix} \Omega_j$$

Furthermore, the term containing  $E_L$  will be more and more enhanced as  $\omega$  gets closer and closer to  $\Omega_j$ . These two important features of the ponderomotive potential are precisely the ones that can give rise to isotope separation.

We would like to particularise our survey to a Neon plasma, composed of the two more abundant isotopes,  $\text{Ne}^{20}$  and  $\text{Ne}^{22}$ , having respectively natural concentrations of 91.2% and 8.8%.

Henceforth, all quantities with index 1 refer to the heavier isotope, while those with index 2 refer to the lighter one.

Let us recall, from an earlier report [2], that the densities can be expressed by :

$$n_j = \beta_j \frac{\tau}{1+\tau} \frac{e^{-\left(\frac{\psi_j}{T_i} + \frac{\psi_e}{T_e+T_i}\right)}}{\sum \frac{\tau}{1+\tau}} \quad (5)$$

in which :

$\beta_j$ : relative proportion of species j

$n_0$ : global density

$T_e, T_i$ : electronic and ionic temperature

$\tau = T_e/T_i$

$$Z = \sum_{j=1}^2 n_0 \beta_j e^{-\frac{\psi_j}{T_i}} \quad (6)$$

It is worth noting that the following two important assumptions allowed us to obtain these expressions from the Boltzmann relation:

- 1) The plasma is considered to be quasi-neutral on length scales much bigger than the Debye's length.
- 2) The ions have the same temperature  $T_i$ , whatever the species may be.

This Neon plasma is bounded by a conducting cylinder, whose radius and height are respectively  $a$  and  $h$ .

The electric field  $E$  must satisfy the boundary conditions :

$$E_{\phi}(a, z) = 0 \quad 0 \leq z \leq h$$

$$E_z(a, z) = 0 \quad 0 \leq z \leq h$$

$$E_r(r, h) = E_r(r, 0) = 0 \quad 0 \leq r \leq a$$

$$E_{\phi}(r, h) = E_{\phi}(r, 0) = 0 \quad 0 \leq r \leq a$$

Our intent is to solve the wave equation :

$$\vec{\nabla} \times \vec{\nabla} \times \vec{E} - \omega^2 \vec{\epsilon}(\vec{E}) \vec{E} = 0 \quad (8)$$

where  $\epsilon$  is the dielectric tensor.

We proved [2] that (8) is Euler's equation of the following problem:

We search for  $E$  and  $\lambda$  that minimise the quantity:

$$J = 2\pi \int_0^1 r dr \int_0^1 dz \left[ \frac{\epsilon^2}{2} + \eta P(\vec{E}) - \frac{\lambda}{2} (\vec{\nabla}_r \times \vec{E})^2 \right] \quad (9)$$

where:

$P(E)$  : total pressure

$\eta$  :  $mn_0/Bo^2$

$s = h/a$  (aspect ratio)

In eq. (9), the linear dimensions have been scaled with the radius a.

Furthermore

$$\lambda = \frac{c^2}{\omega^2 a^2} \quad (\text{M.K.S.}) \quad (10)$$

and

$$\vec{\nabla}_{r_z} \times \vec{E} = \left( \frac{\nu}{r} E_z - \frac{\partial E_\phi}{\partial z}, \frac{\partial E_r}{\partial z} - \frac{\partial E_z}{\partial r}, \frac{1}{r} \frac{\partial(r E_\phi)}{\partial r} - \frac{\nu E_r}{r} \right) \quad (11)$$

since

$$\partial/\partial\phi \rightarrow i\nu$$

As we have no choice for  $\omega$ , that we want as close to the resonance frequency as possible, the actual eigenvalue is the radius a of the cylinder. The nonlinearity lies in the dielectric tensor that has the following density dependence:

$$\vec{\epsilon} = \begin{pmatrix} 1 - \sum_j \frac{\omega_{pj}^2}{\omega^2 - \Omega_j^2} & \sum_j \frac{\omega_{pj}^2 \Omega_j}{\omega(\omega^2 - \Omega_j^2)} & 0 \\ \sum_j \frac{\omega_{pj}^2 \Omega_j}{\omega(\omega^2 - \Omega_j^2)} & 1 - \sum_j \frac{\omega_{pj}^2}{\omega^2 - \Omega_j^2} & 0 \\ 0 & 0 & 1 - \sum_j \frac{\omega_{pj}^2}{\omega^2} \end{pmatrix} \quad (12)$$



where

$$\omega_{pj}^2 = \frac{q_j^2 n_j}{m_j} \quad (13)$$

$$\omega = \frac{q B_0}{\bar{m}} \quad (14)$$

$\bar{m}$  designates the average mass :

$$\bar{m} = 2, \frac{m_1 m_2}{m_1 + m_2} \quad (15)$$

To sum up, we want to solve eq. (9) to find the size of the cylinder and the configuration of  $E$ , subject to the boundary conditions (7), that causes appreciable density modifications. We fix the intensity of the magnetic field  $B_0$ , the aspect ratio of the cylinder, the density  $n_0$ , the frequency  $\omega$  and the temperature ratio  $\tau$ .

### 3. NUMERICAL TREATMENT

#### 3.1 Spectrum of the vacuum operator, elimination of pulluting modes

The choice of an appropriate discretisation shows always to be a rather tricky task. We want to solve the eigenvalue problem, represented by eq. (9) in the rectangular domain :

$$0 < r < 1$$

$$0 < z < 1$$

that corresponds to a meridian plane of the cylinder. Since the operator  $\nabla_{rz} \times E$  contains only derivatives with respect to  $r$  and  $z$ , the centred finite-difference scheme appears to fit quite well. Moreover, as only  $E_\phi$  is derived with respect to both coordinates, according to eq. (13), the arrangement of the eigenvector component over the mesh may be the one shown in fig. 1 having discretised,  $(E_r, rE_\phi, E_z)$ . The mesh is formed with  $m_r$  points in the  $r$ -direction, and  $m_z$  in the  $z$ -direction.

Looking back to equation (9), one can guess the reason of the choice of such an eigenvector. Longitudinal modes, otherwise physically irrelevant, have an infinite eigenvalue, which is infinitely degenerated. Indeed:

$$\begin{cases} \vec{\nabla}_{rz} \times \vec{E} = 0 \\ \lambda \rightarrow \infty \end{cases} \quad (16)$$

is a solution for eq. (9).

It is no accident that the discretisation using the covariant components  $(E_r, rE_\phi, E_z)$  leads to a pollution-free representation of the curl. In fact, the gradient of a function in any coordinate system is a covariant vector whose curl is formally identical to the curl in cartesian coordinates. It is this property which guarantees that the discrete operators curl and gradient satisfy

$$\text{curl}(\text{grad } \psi) \equiv 0$$

for any  $\psi$  thereby assuring

$$\lambda \rightarrow \infty$$

for all longitudinal modes.

From now on, we will dedicate the capital letters to the discretised quantities over all the mesh, while the small ones shall be assigned to the same quantities referred over one elementary cell.

The local numbering on the  $j$ -th cell, is shown in fig. (2).  $\Delta r_j$  and  $\Delta z_j$  are its dimension,  $r_j$  the distance from its centre to the  $z$ -axis.

$x_j$  is then an eight-dimensional vector. Let us call  $t_j$  the operator performing the correspondance between  $x_j$  and the actual electric field evaluated at the centre of the  $j$ -th cell,  $e_j$ .

$$\vec{e}_j = \vec{t}_j \vec{x}_j \quad (17)$$

$$\vec{t}_j = \begin{pmatrix} 0 & \frac{1}{2} & 0 & 0 & 0 & 0 & \frac{1}{2} & 0 \\ \frac{1}{4r_j} & 0 & \frac{1}{4r_j} & 0 & 0 & \frac{1}{4r_j} & 0 & \frac{1}{4r_j} \\ 0 & 0 & 0 & \frac{1}{2} & \frac{1}{2} & 0 & 0 & 0 \end{pmatrix} \quad (18)$$

In the same way, the curl of the electric field may be expressed in terms of  $x_j$  as:

$$\vec{\nabla} \times \vec{e}_j = \vec{w}_j \vec{x}_j \quad (19)$$

in which

$$\vec{W}^j = \begin{pmatrix} \frac{1}{2r^j \Delta z^j} & 0 & \frac{1}{2r^j \Delta z^j} & \frac{r^j}{2r^j} & \frac{r^j}{2r^j} & \frac{-1}{2r^j \Delta z^j} & 0 & \frac{-1}{2r^j \Delta z^j} \\ 0 & \frac{-1}{\Delta z^j} & 0 & \frac{1}{\Delta r^j} & \frac{-1}{\Delta r^j} & 0 & \frac{1}{\Delta z^j} & 0 \\ \frac{1}{2r^j \Delta r^j} & \frac{-r^j}{2r^j} & \frac{1}{2r^j \Delta r^j} & 0 & 0 & \frac{-1}{2r^j \Delta r^j} & \frac{-r^j}{2r^j} & \frac{1}{2r^j \Delta r^j} \end{pmatrix} \quad (20)$$

With these definitions, the discretised form of eq. (9) becomes

$$\begin{aligned} \chi &= \sum_{j=1}^{m_s} \left[ \vec{e}^j \cdot \vec{\varepsilon}^j \vec{e}^j - \lambda \left( \vec{v}_{r_z}^j \times \vec{E}^j \right)^2 \right] \pi r^j \Delta r^j \Delta z^j \\ &= \sum_{j=1}^{m_s} \left( \vec{x}^j \cdot \vec{e}^j \vec{\varepsilon}^j \vec{e}^j \vec{x}^j - \lambda \vec{x}^j \cdot \vec{w}^j \vec{w}^j \vec{x}^j \right) \pi r^j \Delta r^j \Delta z^j \\ &= \sum_{j=1}^{m_s} \left( \vec{x}^j \cdot \vec{a}^j \vec{x}^j - \lambda \vec{x}^j \cdot \vec{b}^j \vec{x}^j \right) \pi r^j \Delta r^j \Delta z^j \\ &= \vec{X} \cdot \left[ \vec{A}(\vec{X}_0) - \lambda \vec{B} \right] \vec{X} \end{aligned}$$

$$m_s = (m_r - 1) \cdot (m_z - 1)$$

Setting the variation with respect to  $\vec{X}$  equal to zero

$$\left[ \vec{A}(\vec{x}_0) - \lambda \vec{b} \right] \vec{x} = 0 \quad (21)$$

Once this stage is reached, one may examine the spectrum of the operator, try to classify and identify the modes.

The propagation of electromagnetic waves within a hollow cylinder (wave guide) may be investigated in the same way, dropping only the density to zero. In that case, the operator A depends no longer on  $x_0$ . The spectrum obtained has to be compared to the well-known TE and TM modes propagating into a wave-guide, and this is shown in fig. (3). The computation has been done by an eigenvalue solver routine, called Vekit, part of the code ERATO [5], and with the following parameters:

$$\begin{array}{ll} m_r = 4 & \omega = 4.55 \text{ MHz} \\ m_z = 4 & \nu = 1 \\ s = 25 & B_0 = 1.7 \end{array}$$

Every mode may be denominated by its azimuthal number  $\nu$ , and its radial and axial numbers,  $\ell_r$  and  $\ell_z = \text{TE}_{\nu \ell_r \ell_z}$

For example :

TE<sub>112</sub>

designates the first transverse electric mode, having one wavelength in the axial direction, with  $v = 1$ .

Let us set down the items of the modes:

Expected modes:

$$\begin{array}{ll}
 \text{TE} & m_r m_z - 2m_r - m_z + 2 \\
 \text{TM} & m_r m_z - m_r - m_z + 1 \\
 \text{boundary conditions} & \underline{4m_r + 3m_z - 7} \\
 N_i = & 2m_r m_z + m_r + m_z - 4
 \end{array} \tag{22}$$

If we subtract this quantity from the total number of variables

$$N_v = 3m_r m_z - m_r - m_z \tag{23}$$

we get

$$N_g = N_v - N_i = m_r m_z - 2m_r - 2m_z + 4 \tag{24}$$

$N_g$  is precisely the number of infinitely degenerated eigenvalue corresponding to the gradient modes. Indeed, the boundary conditions impose on the electrostatic potential  $U$  to take null values on the cylinder surface and on the axis, as illustrated in fig. (4). So, only the values of  $U$  taken on the internal modes are independent, and the mesh has exactly

$$N_g = (m_r - 2) (m_z - 2)$$

internal points.

### 3.2 Iteration method to solve the nonlinear equation

This section is dedicated to the setting forth of the iterative process. We propose here the association of two methods, that allows us to reach acceptable amplitudes for the electric field.

An auxiliary condition to eq. (9) may be suggested by physical considerations. Indeed, as the eigenvalue is modified, the volume of the cylinder is actually changed.

Let us recall that, since  $a$  is related to  $\lambda$  by means of eq. (10), the volume of the box is given by:

$$V = \pi \omega^{-3} \lambda^{-3/2} a \quad (25)$$

But the average density of each species,  $\bar{n}_j$ , must be kept fixed. At each step, we must then compute the relative number of particles of each species,  $\beta_1, \beta_2$ , in order to ensure that:

$$\bar{n}_j = \frac{N_j}{V} = \text{constant} \quad (26)$$

When the iterative process begins,  $\beta_1$  and  $\beta_2$  are obviously equal to the natural concentrations

$$\begin{aligned} \beta_1^0 &= 8.8\% \\ \beta_2^0 &= 91.2\% \end{aligned} \quad (27)$$

The chosen method for solving eq. (9) consists of 2 steps:

- i) We first set  $\vec{X}_0$  to zero and solve the nonlinear eigenvalue equation iterating:

$$\left[ \vec{A}(\vec{X}_{n-1}) - \lambda_n \vec{B} \right] \vec{X}_n = 0 \quad (28)$$

We impose the condition that the electric field adjusts itself so that the exponent of  $n_2$  reaches a maximum fixed value  $\psi_{2M}$  in one point.

$$\vec{X}_n = \vec{X}_n^1 \left( \gamma \psi_{2M} \right)^{1/2} \quad (29)$$

where  $\vec{X}_n^1$  designates the eigenvector having norm 1 at the step  $n$ , and  $\gamma$  a proportionality factor.

This method converges well only for small values of  $\psi_{2M}$ . For this reason, a predictor-corrector method was used which is described in the next section.

- ii) Eq. (21) can be written as:

$$f(\lambda, \vec{x}) = 0 \quad (30)$$

Supposing one solution to be known as  $(\lambda_0, \vec{x}_0)$ , we can expand eq. (30) around this point:

$$f(\lambda, \vec{x}) = f(\lambda_0, \vec{x}_0) + \frac{\partial f}{\partial \lambda} \bigg|_{(\lambda_0, \vec{x}_0)} \Delta \lambda + \frac{\partial f}{\partial \vec{x}} \bigg|_{(\lambda_0, \vec{x}_0)} \Delta \vec{x} + \dots$$



The first term of the right-hand side is zero, so:

$$\Delta \vec{x} = \left[ \frac{\partial f}{\partial \vec{x}} \bigg|_{(\lambda_0, \vec{x}_0)} \right]^{-1} \frac{\partial f}{\partial \lambda} \bigg|_{(\lambda_0, \vec{x}_0)} \Delta \lambda \quad (31)$$

A rough approximation to the solution,  $\vec{x}'$  is thus predicted by Euler's method:

$$\vec{x}' = \vec{x}_0 + \Delta \vec{x} \quad (32)$$

Holding  $\lambda = \lambda_0 + \Delta \lambda$  constant, Newton's method applied to

$$g_\lambda(\vec{x}) = f(\lambda, \vec{x}) \quad (33)$$

will correct  $\vec{x}'$ . Let us expand eq. (33) around  $\vec{x}'$ :

$$g_\lambda(\vec{x}_{n+1}) = g_\lambda(\vec{x}_n) + \frac{\partial g_\lambda}{\partial \vec{x}} \bigg|_{\vec{x}_n} \Delta \vec{x}_{n+1} \quad (34)$$

with

$$\vec{x}_1 = \vec{x}'$$

Consequently:

$$\vec{x}_{n+1} = \vec{x}_n - \left[ \frac{\partial g_\lambda}{\partial \vec{x}} \bigg|_{\vec{x}_n} \right]^{-1} g_\lambda(\vec{x}_n) \quad (35)$$

If we apply eq. (31) and Eq. (35) to eq. (21), we obtain:

$$\vec{X}' = \vec{X}_0 + \left[ \vec{A}(\vec{X}_0) - \lambda_0 \vec{B} + \mathcal{D}(\vec{X}_0) \right]^{-1} \Delta \lambda \vec{B} \vec{X}_0 \quad (36)$$

$$\vec{X}_{n+1} = \vec{X}_n + \left[ \vec{D}(\vec{X}_n) - \lambda \vec{B} \right]^{-1} \left[ \vec{A}(\vec{X}_n) - \lambda \vec{B} \right] \vec{X}_n \quad (37)$$

in which

$$\vec{D}_{ij} = \frac{\partial A_{i-k}}{\partial X_j} \vec{X}_k \quad (38)$$

The growth of the amplitude is then driven by the step  $\Delta \lambda$  assigned to the parameter  $\lambda$ . Inch by inch, we may then compute the curve  $\psi_{2M}(\lambda)$  (Fig. 6).

This method was widely described by Keller [6].

#### 4. NUMERICAL RESULTS

With a regular mesh defined by:

$$m_r = 11$$

$$m_z = 11$$

$$s = 10$$

eq. (9) is solved for the normalised electric field:

$$\vec{E} = \zeta^{-1} \vec{E} \quad (41)$$

where

$$\zeta = \frac{B_0^2 T_i}{\bar{m}} \quad (42)$$

The frequency  $\omega$  is arbitrarily taken as the mean value of the two cyclotron frequencies. Since, from eq. (15), for a Neon plasma  $m$  has the value

$$m = 3.5 \cdot 10^{-26} \text{ kg} \quad (43)$$

this gives for  $\omega$

$$\omega = 4.56 \text{ MHz} \quad (44)$$

For a specific example, we have chosen the following physical values

$$B_0 = 1 \text{ Tesla}$$

$$n_0 = 10^{16} \text{ m}^{-3}$$

$$T_i = 1 \text{ eV}$$

$$\tau = 5$$

In accordance with eq. (42) we obtain for the normalisation of the electric field :

$$\xi = 2.141 \text{ kV/m}$$

The results of the first step are shown in fig. (5a) and (5b). The amplitude reached is not considerable, so that density variations are too weak to deserve to be plotted. Nevertheless, these plots are interesting by the fact they depict approximately the amplitude profiles. We have restricted our work to the most simple mode, that presents one null for  $E_r$  in the radial direction, while  $E_z$  has one null in the axial direction.

The predictor-corrector methods leads to the results shown in the next figures. The growth  $\lambda$  is controlled by

$$\lambda = \lambda_0(1 + \delta) \quad (45)$$

with

$$\lambda_0 = 3700.$$

Figs. (6), (7) and (8) represent quite well the progression of three important parameters  $\psi_{2M}$ ,  $\beta_1$  and  $\beta_2$  with respect to  $\delta$ .

The process stops for  $\delta \approx .22$ , the convergence at that stage becoming difficult: although the number of iterations of the Newton's approximation is very low, the step gets narrower. Nevertheless, the corresponding value of  $\psi_{2M} \approx 2.2$  is quite satisfactory. The plot of  $\beta$  seems also to saturate whereas  $\beta_2$  decreases almost linearly.

Fig. (9) through fig. (12) show the final results. The axial and radial profiles of the electric field are sketched in figs. (9) and (10). One may notice that the slope of  $E_r$  and  $E_\phi$  becomes stiffer as one moves towards the axis, whereas in fig. (5a), the profiles were smoother.

We can see that the lighter atoms accumulate near the edge and in the middle of the box, while the heavier ones bunch rather on the axis. The ponderomotive force acts little on electrons, except near the axis and the end plates.

## 5. CONCLUSION

We found solutions of large amplitude for the nonlinear wave equation within the frame of the ideal three-fluid theory. With this end in view, we have neglected the effect of collisions but in a precedent paper [2], we have given the conditions under which collisions do not broaden noticeably the resonances.

Moreover, the stability of such solutions has to be investigated to ensure their physical existence; it will be the subject-matter of a forthcoming report.

## ACKNOWLEDGEMENT

The authors wish to express their thanks to Dr. J. Rappaz for the fruitful discussions on the predictor-corrector method.

This report has been supported by the Ecole Polytechnique Fédérale de Lausanne, by the Swiss National Science Foundation and by Euratom.

## REFERENCES

- [1] M.C. Festeau-Barrioz and E.S. Weibel, Phys. Fluids 23, 2045 (1980)
- [2] E.S. Weibel and M.C. Festeau-Barrioz, Plasma Physics (to be published)
- [3] E.S. Weibel, Am. J. Phys. 36, 1130 (1968)
- [4] H. Motz and C.J.M. Watson, Adv. Electron. Electron. Phys. 23, 153 (1967)
- [5] R. Gruber, F. Troyon, D. Berger, L.C. Bernard, S. Rousset, R. Schreiber, W. Kerner, W. Schneider, K.V. Roberts, Computer Phys. Com. 21, 323 (1981)
- [6] Herbert B. Keller, Numerical solutions of bifurcation and non-linear eigenvalue problems, Proc. of an advanced seminar conducted by the Mathematics Research Center, University of Wisconsin at Madison, October 1976  
(edited by Paul H. Rabinowitz)

## FIGURE CAPTIONS

Figure 1: Mesh for the finite-difference scheme

Figure 2: Local numbering on the  $j$ -th cell

Figure 3: Comparison between theoretical waveguide spectrum and the modes obtained in a numerical way

Figure 4: Local arrangement for the electrostatic potential  $U$  on the  $j$ -th cell

Figures 5a and 5b:

The electric field  $E_r$ ,  $E_\phi$ ,  $E_z$  as a function of the radius  $r$ , and the height  $z$  obtained by solving the eigenvalue equation. The electric field is measured in units of  $\sqrt{T_i/m_i} B_0$  and the distance in units of 1.08m.

Figure 6: Progression of  $\psi_{2M}$  as a function of  $\delta$

Figure 7: Progression of  $\beta$  as a function of  $\delta$ . One may notice the saturation appearing at  $\approx .18$

Figure 8: Progression of  $\beta_2$  as a function of  $\delta$

FIGURE CAPTIONS (cont'd)

Figures 9 and 10:

The electric field  $E_r$ ,  $E_\phi$ ,  $E_z$  as a function of the radius  $r$  and the height  $z$  obtained by the predictor-corrector method, for  $\delta = 2.2$ . The electric field is measured in units of  $\sqrt{T_i/m_i} B_0$ , and the unit distance is .967m. The mesh used is  $m_r = 11 = m_z$  and  $s = 10$

Figure 11: The density variation of the minority species  $Ne^{22}$  as a function of  $r$  and  $z$

Figure 12: The density variation of the majority species  $Ne^{20}$  as a function of  $r$  and  $z$



$\times E_r$   
 $\circ r^E \phi$   
 $\Delta E_z$

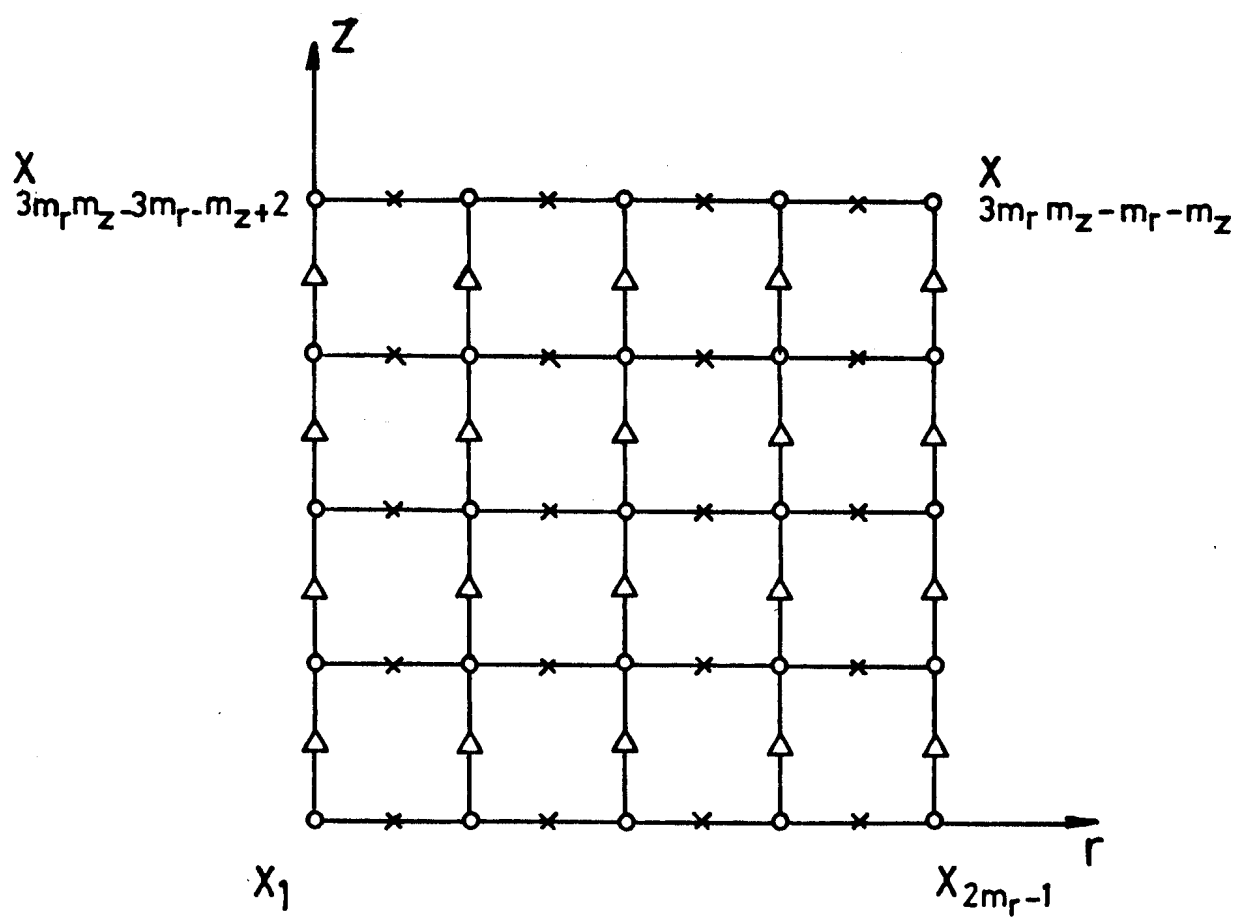


Fig. 1

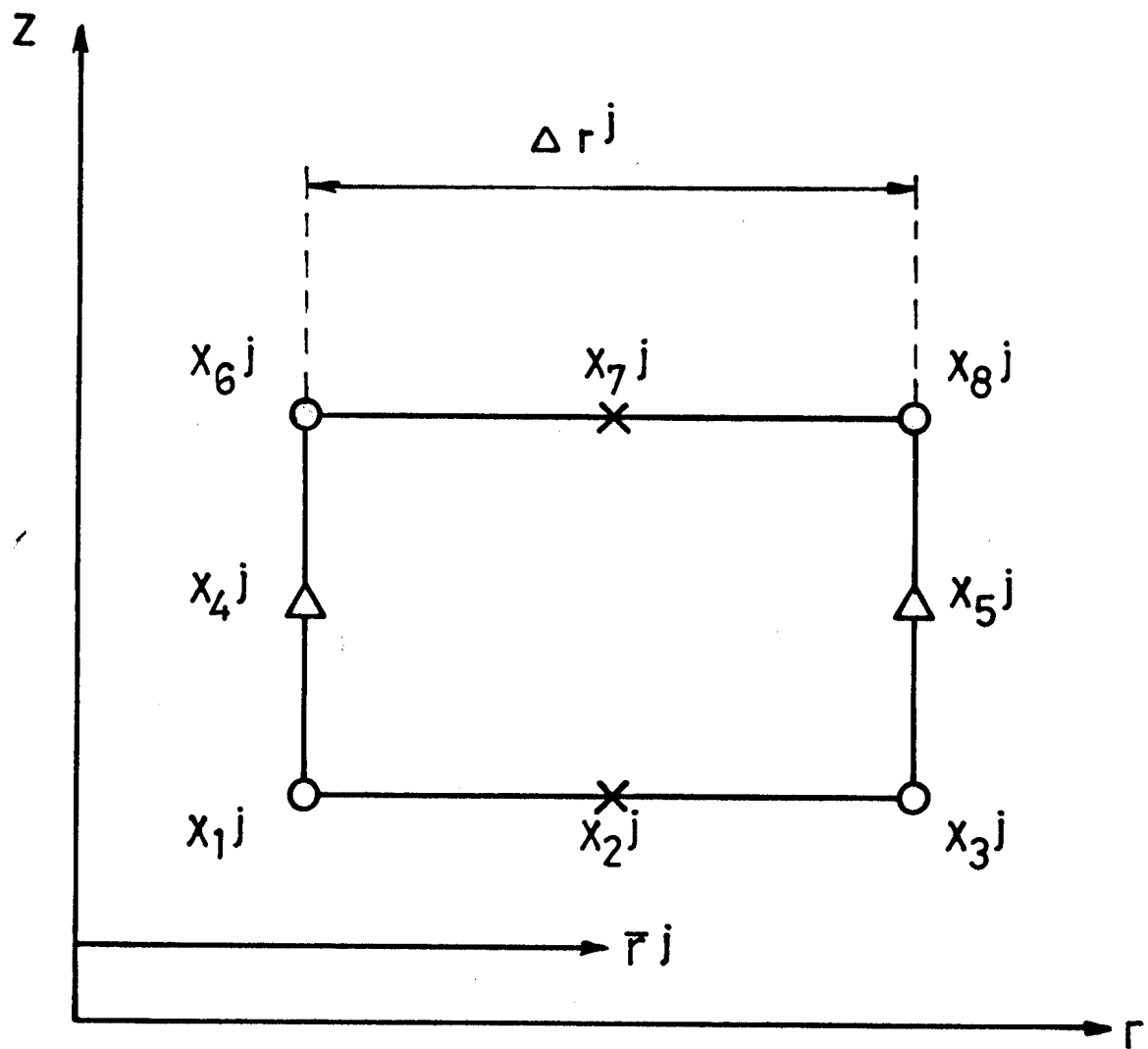


Fig. 2

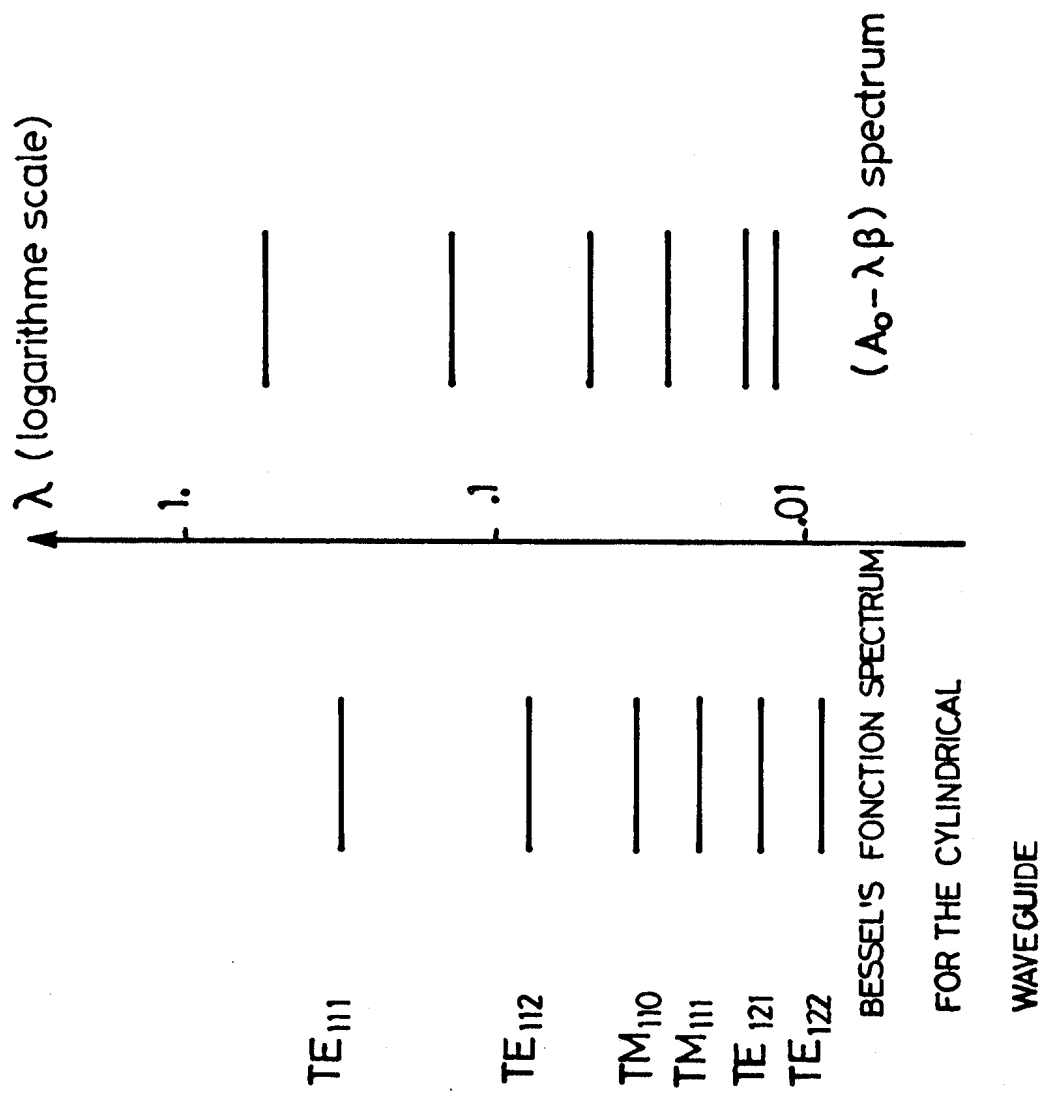


Fig. 3

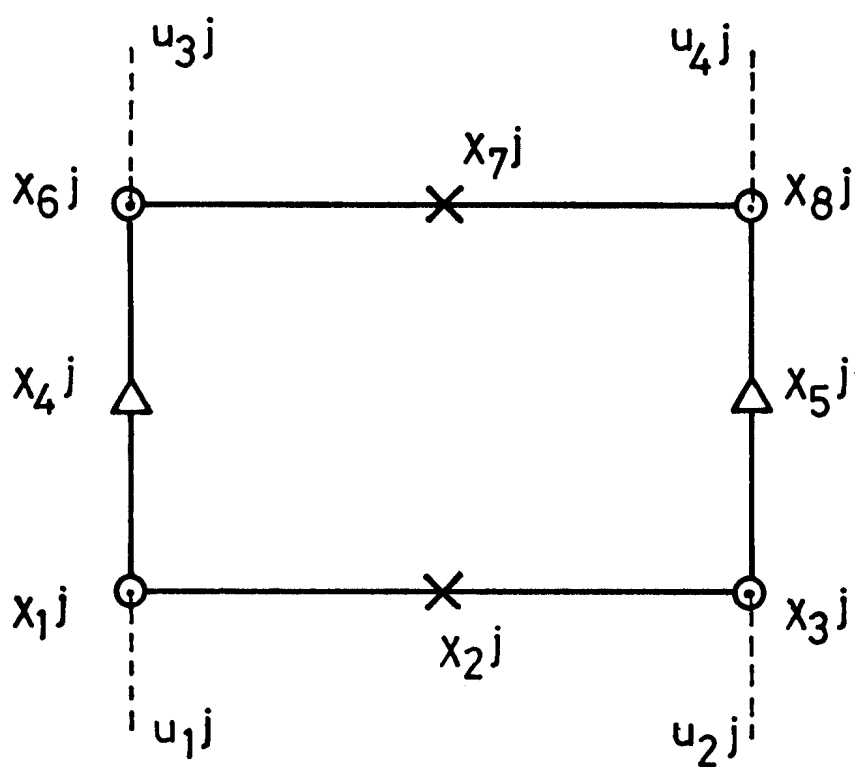


Fig. 4

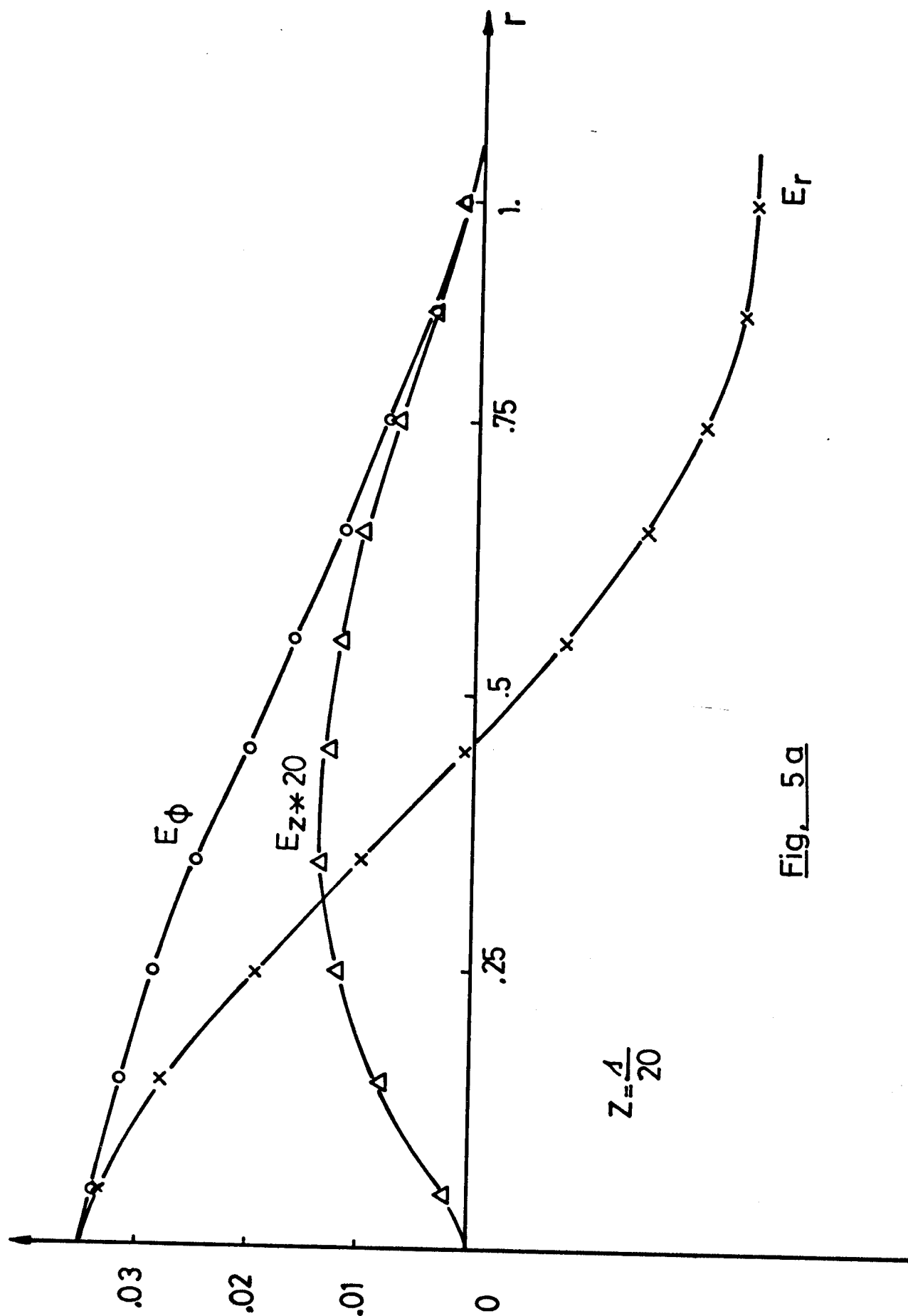


Fig. 5a

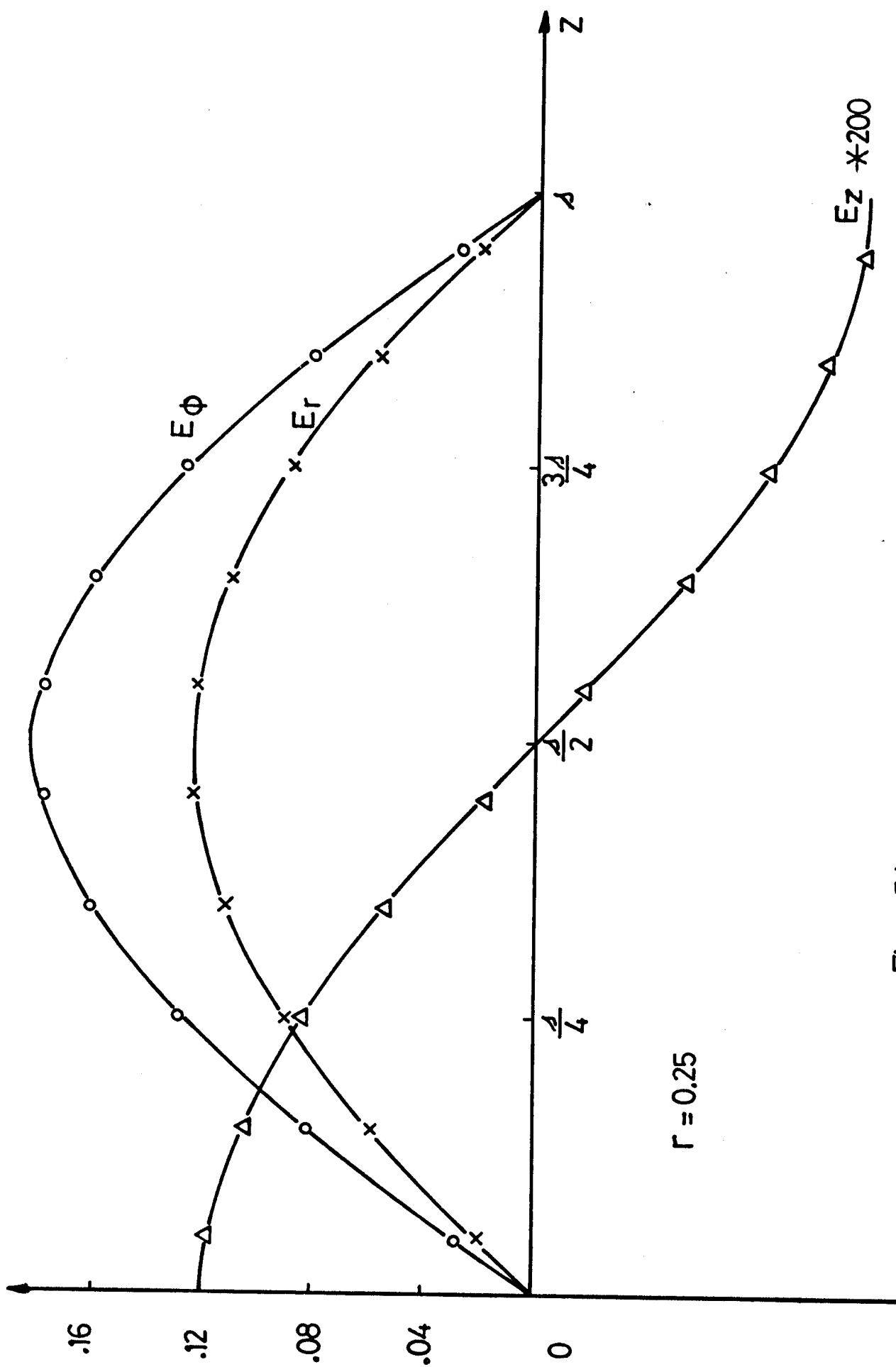


Fig. 5b

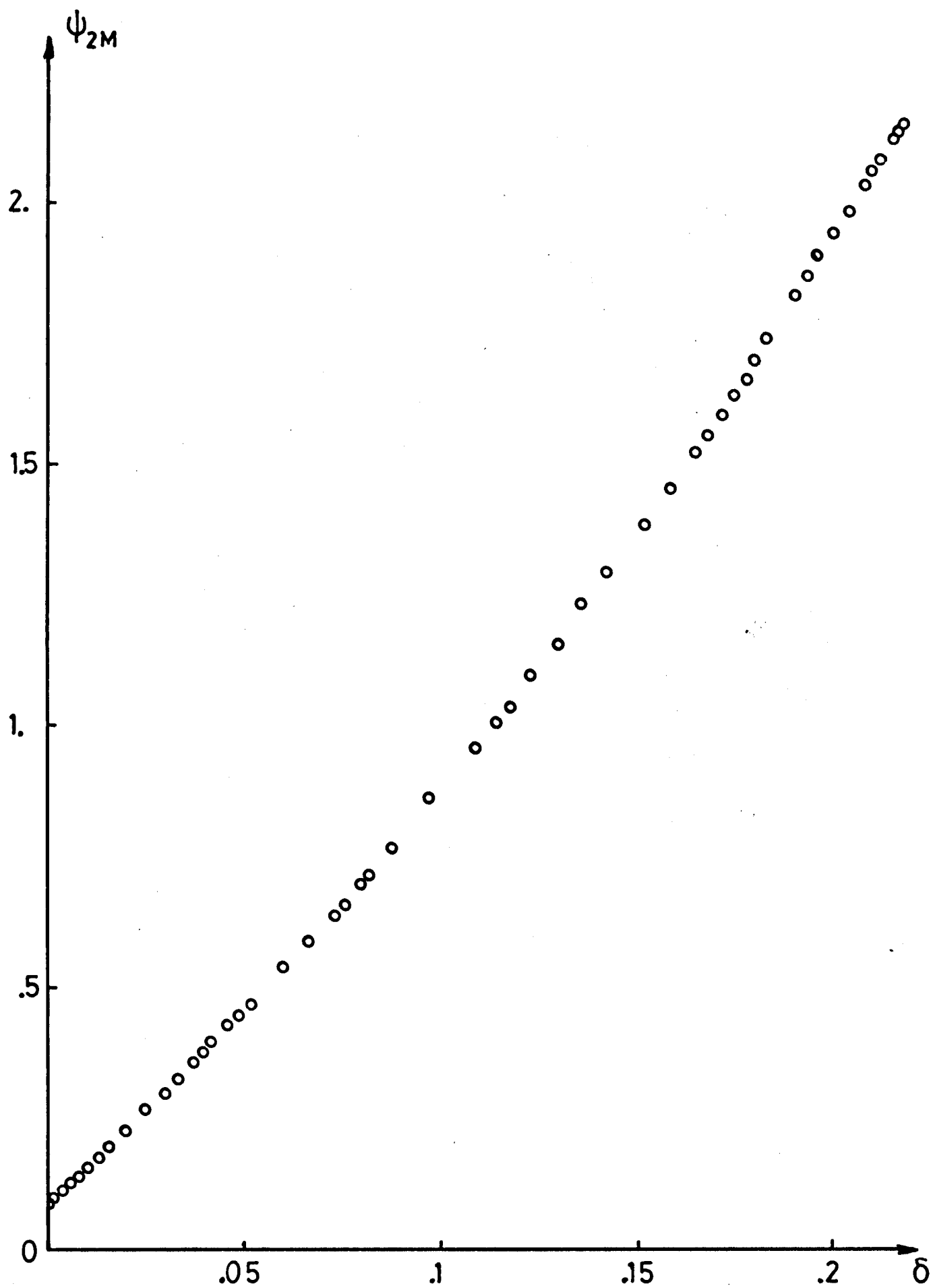


Fig. 6

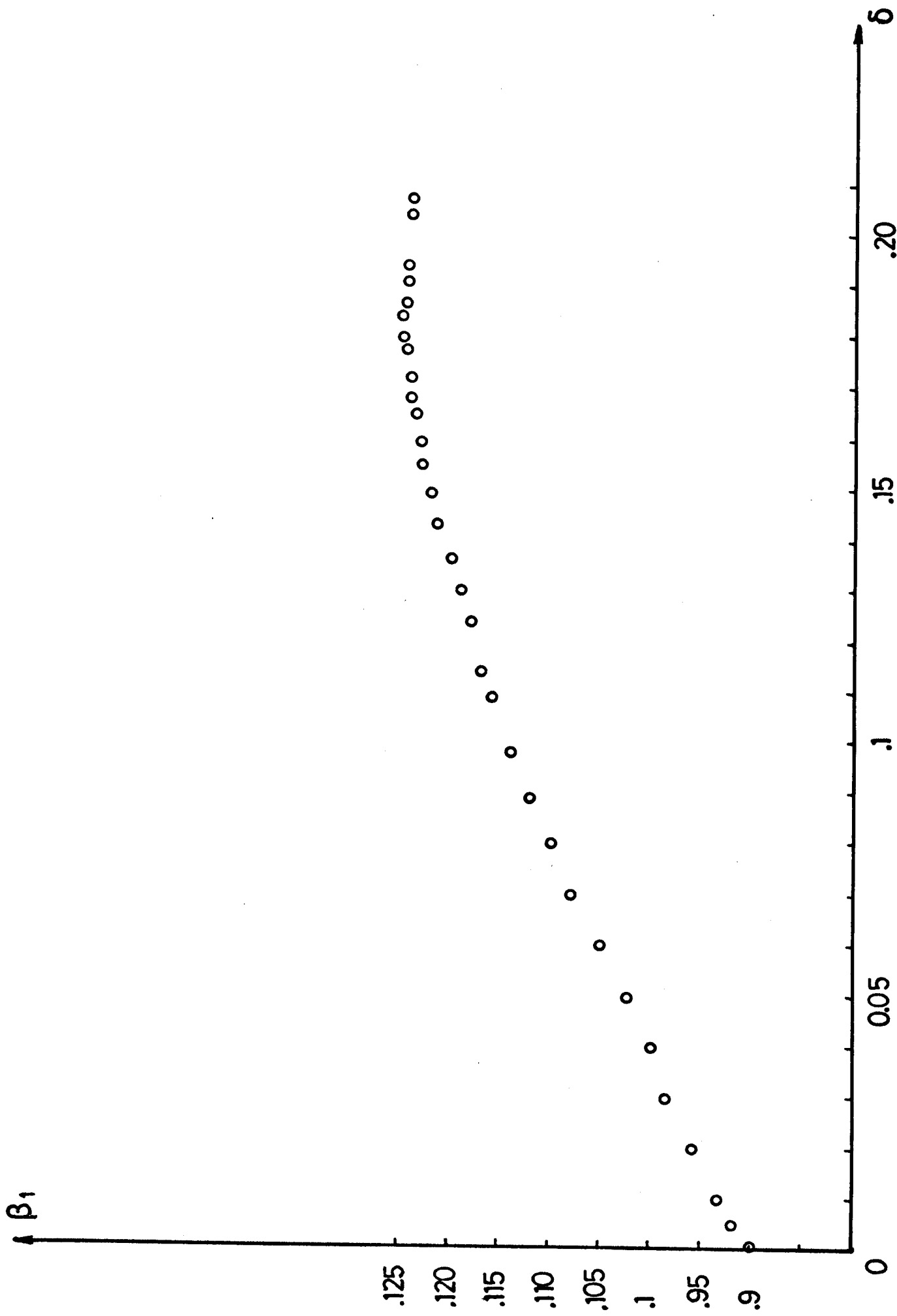


Fig. 7



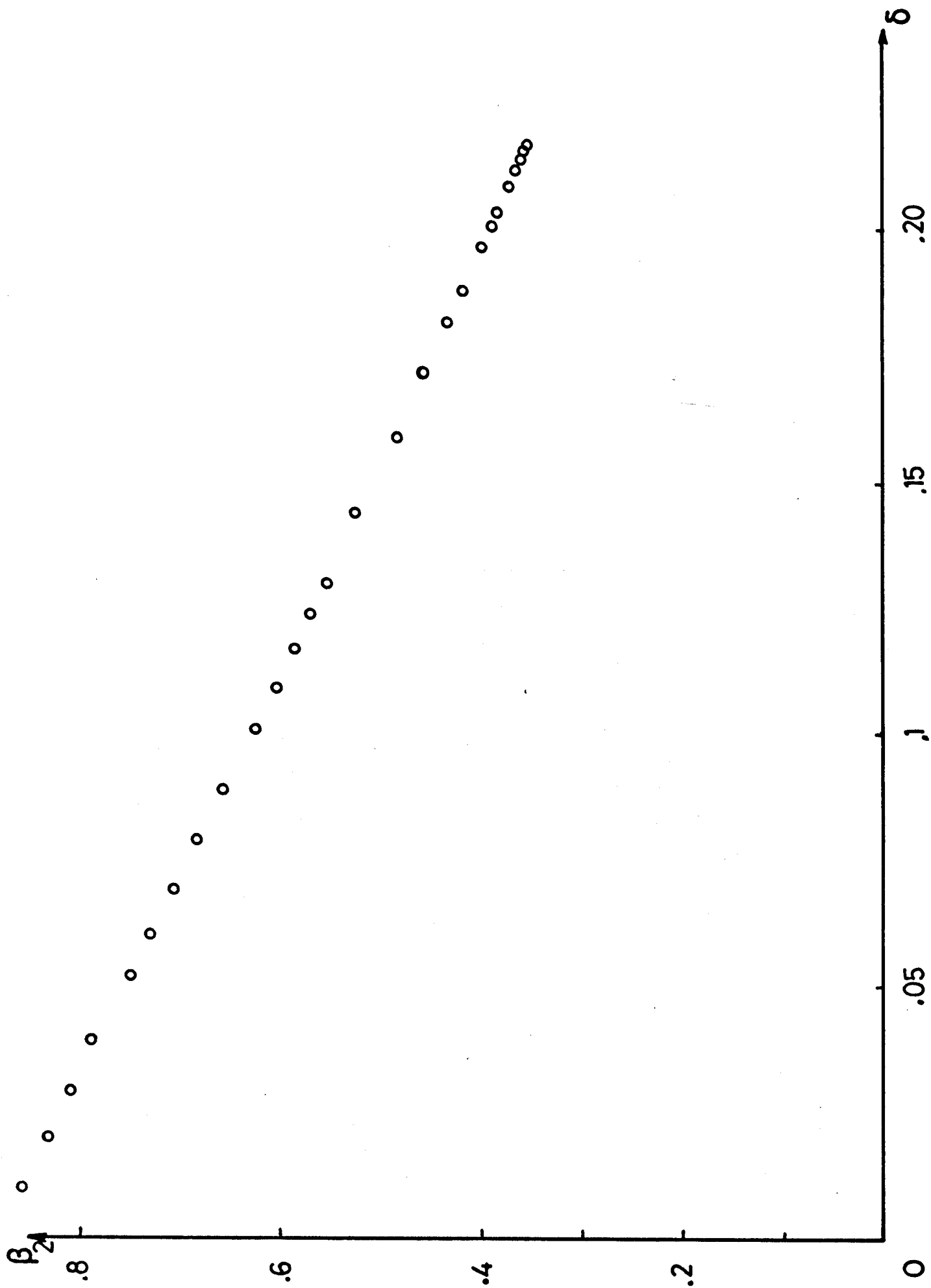


Fig. 8

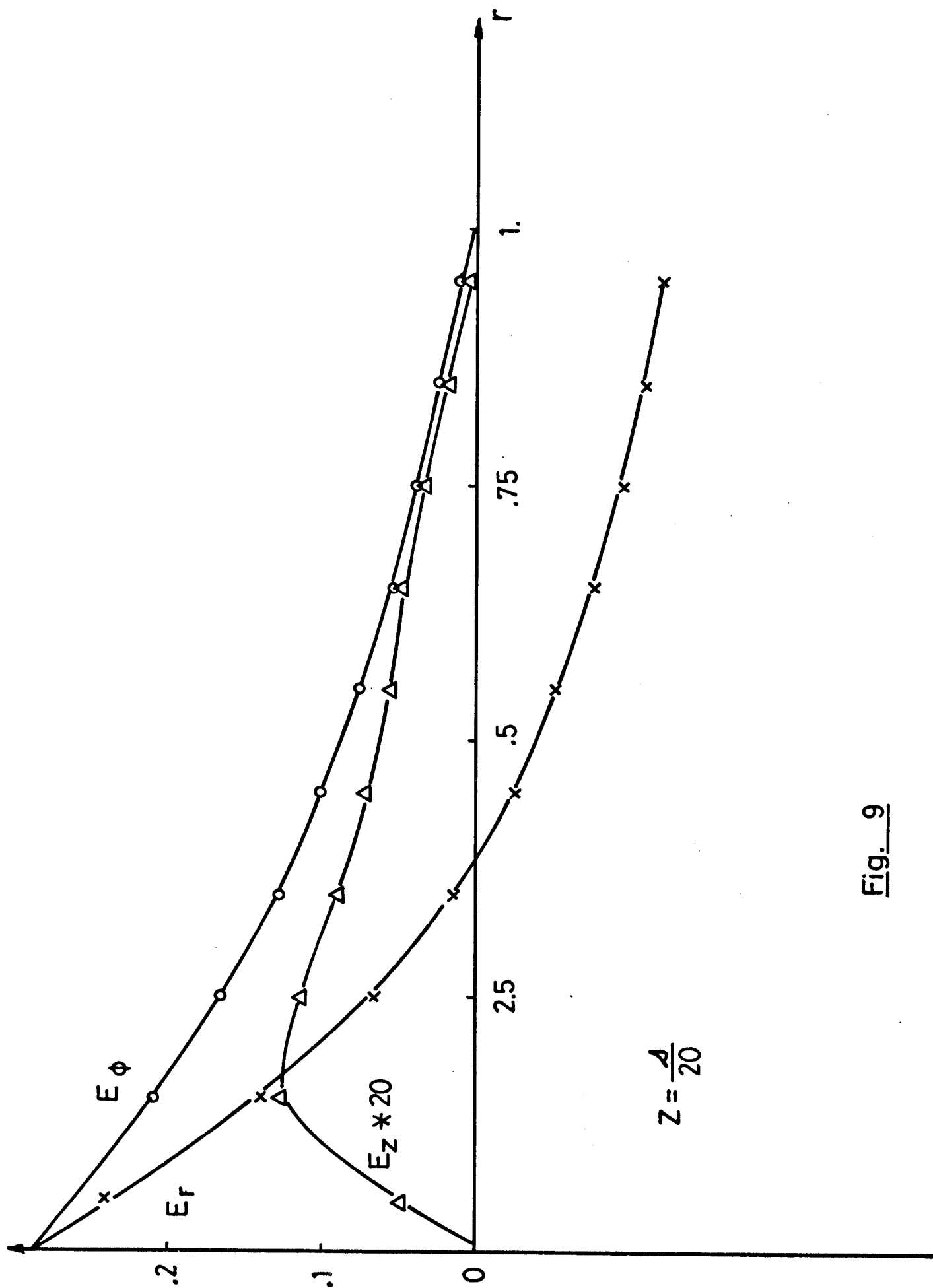


Fig. 9

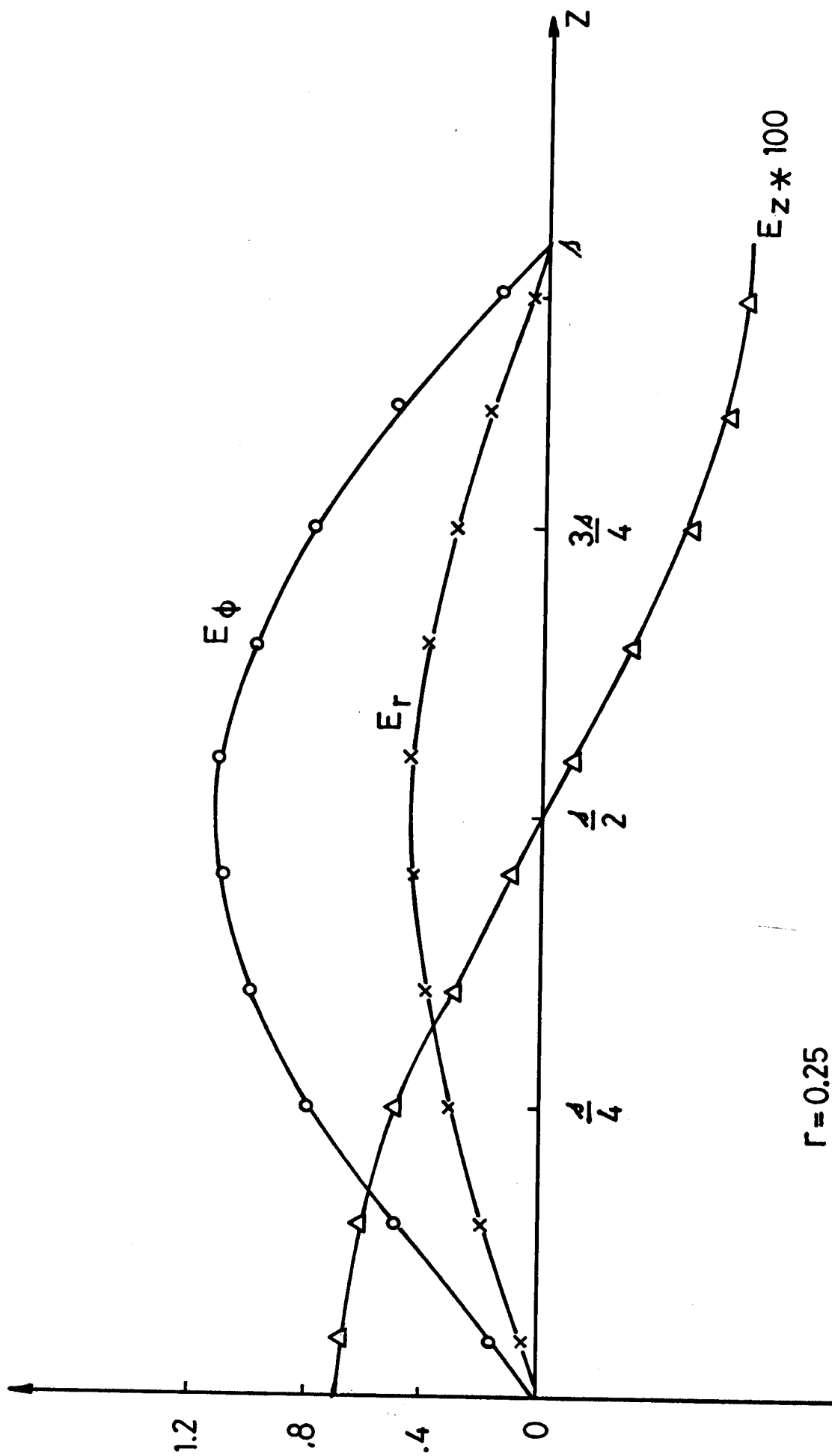


Fig. 10

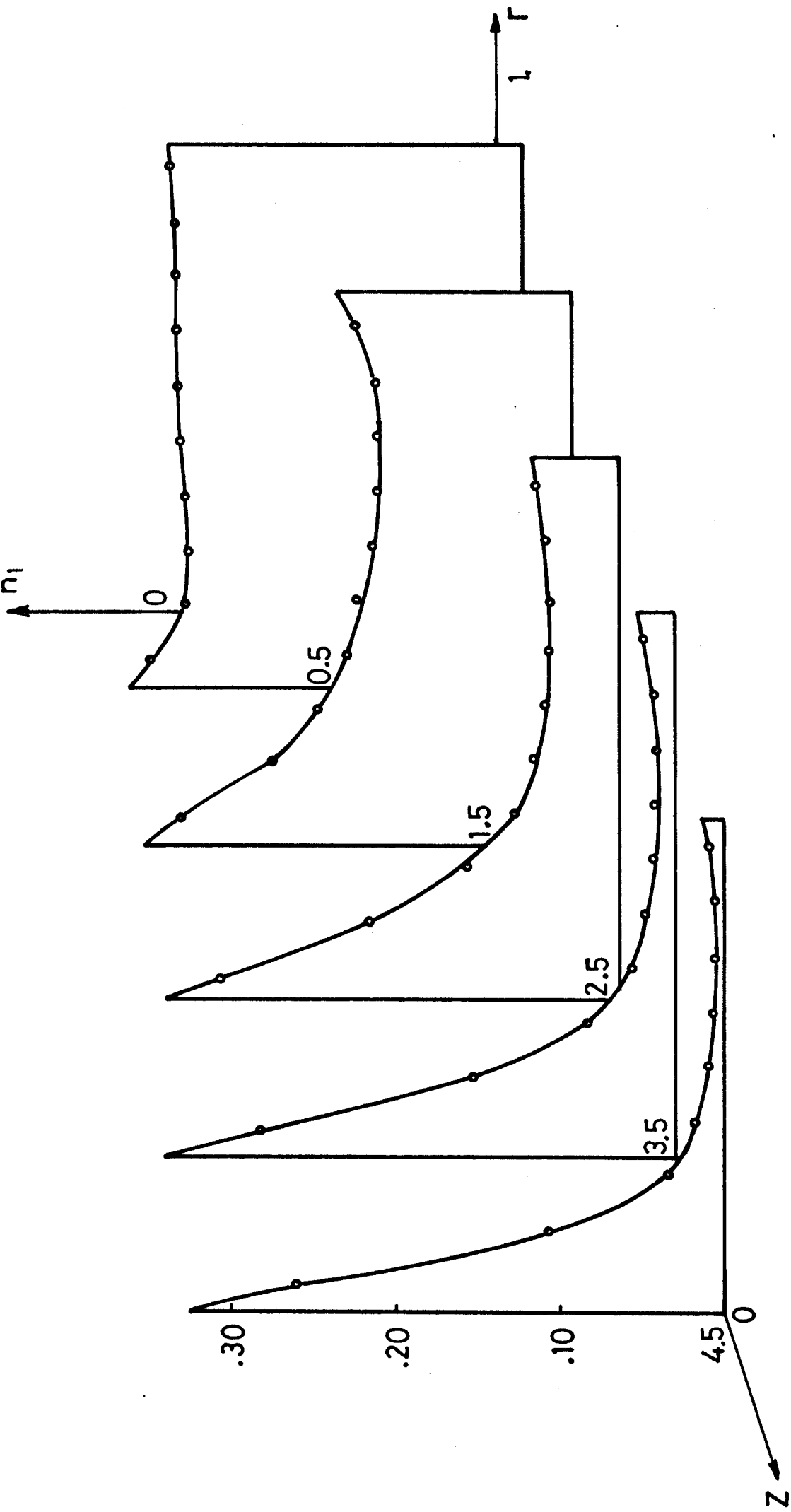


Fig. 11

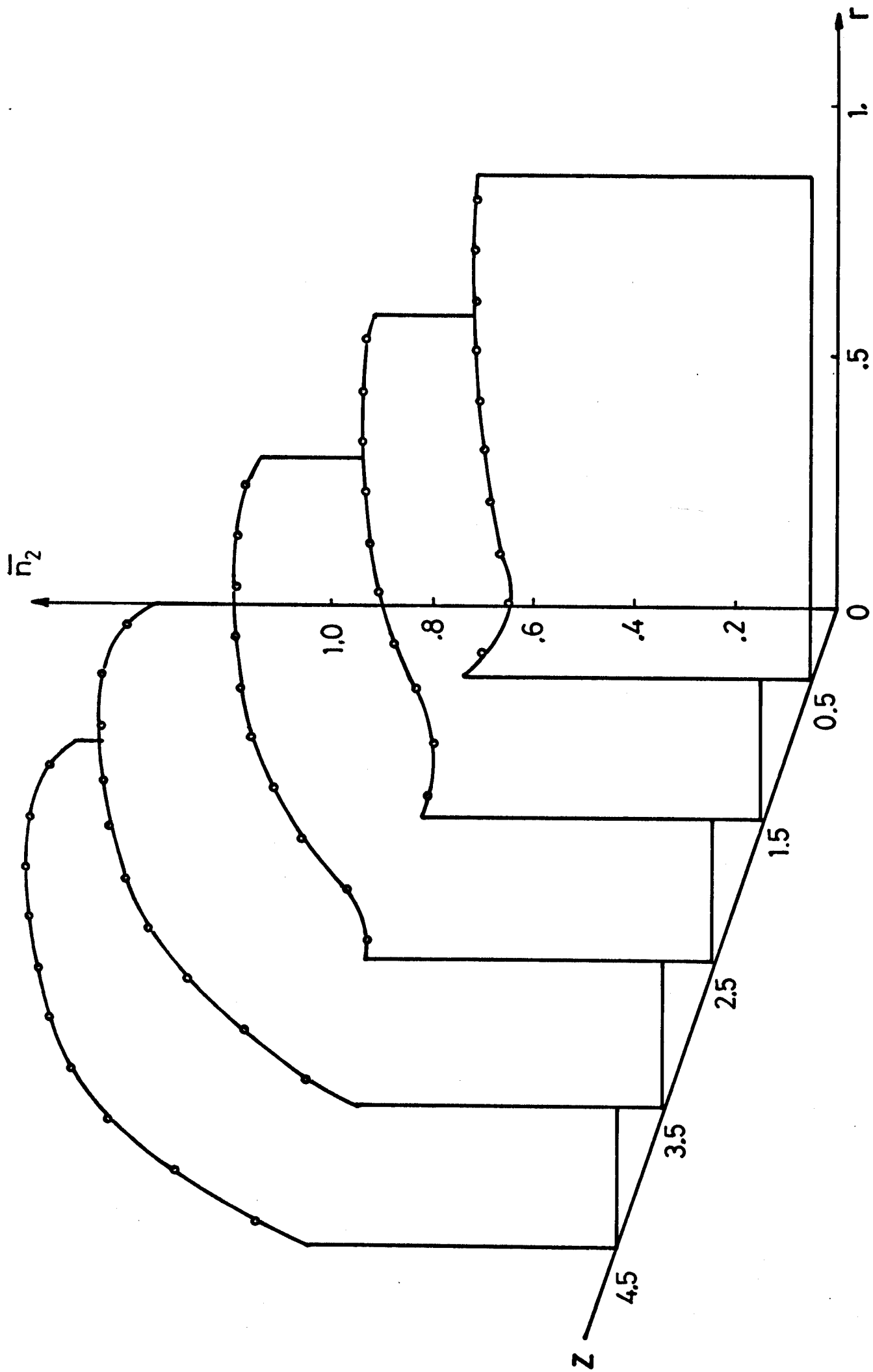


Fig. 12